J Mater Sci (2011) 46:1021–1026
DOI 10.1007/s10853-010-4867-8

Methylthiolate adsorbed on as-rich GaAs (001) surface

W. Gao · S. E. Zhu · M. Zhao

Received: 4 May 2010 / Accepted: 23 August 2010 / Published online: 11 September 2010
© Springer Science+Business Media, LLC 2010

Abstract The adsorption of the methylthiolate (MT) on the as-rich GaAs (001) surface has been studied by using density functional theory (DFT) calculations with a three-dimensional periodic boundary condition. A complete characterization of structures and binding energies of the system consisting of MT and As-rich GaAs (001) surface is obtained. It is found that the most reactive binding site is related to empty Ga dangling bonds located at the three-fold-coordinated second-layer Ga atom. Moreover, electronic properties of these structures are also calculated to study the bonding characteristics of S–Ga and S–As bonding, which show that the covalent bonding of the former is stronger than that of the latter. The analysis for this shortest chain binding is helpful to realize the electrical passivation and chemical protection of GaAs surfaces.

Introduction

Self-assembled monolayers (SAMs) of organosulfur compounds on semiconductor surfaces have attracted a great deal of interests from both fundamental perspectives and potential applications in recent years [1, 2]. GaAs as a promising III–V compound semiconductor has excellent bulk characteristics with direct band gap and high carrier mobility [1, 3]. The absence of commercial GaAs-based high-powered electronic devices can be attributed to the poor thermal oxidation property and electronic passivation characteristics. Formation of SAMs on semiconductor surfaces, together with the potential of this approach for efficient surface passivation, has been demonstrated [4–6]. Other potential applications of SAMs on semiconductor surfaces, particularly on GaAs, are the creation of transition layers for ohmic contacts and Schottky diodes [7, 8], and the development of GaAs–thiolate interfaces for chemical sensing and biosensing applications [9].

Self-assembled monolayers (SAMs) on Au surfaces have been extensively studied [10–12], which included structural phase diagrams of SAMs as functions of temperature and coverage, the specific structural features of SAMs on a molecular level, and the effect of changes of the molecular backbone and the end group on SAMs structure. There are also some works on SAM formation on GaAs surfaces using alkanethiols [5, 7, 13] and aromatic thiols [14]. The formation of SAMs on GaAs is very sensitive to experimental conditions employed [5]. The reported monolayer structures are therefore different. A detailed analysis of the bonding of the thiol molecules to substrates is critical to understand behaviors of these films [15]. However, the nature of the bonding between GaAs substrate and alkanethiolate remains controversial, where the binding is considered via Ga–S [16], As–S [2], both Ga–S and As–S bonding [17, 18], and even bonding of neither Ga–S nor As–S, due to indirect means and limitations in the instrumental resolution [5]. In order to illustrate the performance changes of GaAs (001) surface that accompanies a molecular self-assembly, this contradiction needs to be solved. However, little information available from the well-studied SAMs of thiolates on noble metals can be applied to GaAs when it is considered a prototype example of SAMs. Moreover, theoretical and experimental predictions on the adsorption site and preference surface bonding keep uncertain [5, 17, 18]. The structure of thiolates adsorbed on GaAs (001) is also difficult to determine experimentally because there exist

W. Gao · S. E. Zhu · M. Zhao (✉)
Key Laboratory of Automobile Materials (Jilin University), Ministry of Education, and School of Materials Science and Engineering, Jilin University, Changchun 130022, China
e-mail: zhaoming@jlu.edu.cn

complicated surface chemistry of GaAs, strong propensity to form oxides with exposure to ambient, and various sources of experimental error [5]. Even for the simplest thiolate, the adsorption property of methylthiolate (MT) on GaAs is not very clear yet. On the GaAs (001) surface, experiments have found that the structure of MT on Ga site is more stable than that of MT on As site [19]. However, the calculated results on As-rich GaAs (001) show that the most stable structure is MT being bonded covalently to As atom [20]. It is also suggested by density functional theory (DFT) calculations that MT is adsorbed at an As atom constituting dimer on GaAs (001) cluster, while the H atom is adsorbed at a Ga atom bonded to this As atom [21]. Thus, it is necessary to further investigate MT/GaAs (001) systems to clarify the above difference. For comparison purpose, the As-rich GaAs (001) will be considered.

It is well known that GaAs (001)-(2×4) reconstruction with the As-rich surfaces has several stable phases, namely, structural models α, β, γ, $\beta2$, and $\alpha2$ [22–29]. Moreover, their electronic and geometry structures are also largely influenced by adsorbates, such as Sb dimmer [30]. α and β phases have the common $\beta2(2\times4)$ structure determined by the combined reflectance difference spectroscopy (RDS) and reflection high-energy electron diffraction (RHEED) analysis [26], and by X-ray diffraction (XRD) studies [31, 32]. DFT calculations have shown that $\alpha2(2\times4)$ structure is the most stable one in an extremely narrow range of As chemical potential [33, 34], while core-level photoemission and scanning tunneling microscopy (STM) works have also supported to the existence of $\alpha2$ domains [27]. Considering the change in RDS, the fraction of $\alpha2$ structure in α phase increases with increasing temperature, and the pure $\alpha2$ phase could not be obtained even at the higher end of the temperature region of the (2×4) phase at 873 K [26, 28]. Using STM, $\alpha2$ domains appear after heating $\beta2$ surface under ultra high vacuum condition [28]. Thus, $\alpha2(2\times4)$ structure could not be thermodynamically stable and may only be reached through appropriate kinetic pathways [28]. As discussed above, GaAs (001)-(2×4) surface consists of the well-ordered $\beta2$ structure in a relatively wide range of substrate temperature under As fluxes. Although other structures, such as β, α, and $\alpha2$, could also be formed under actual experimental conditions, they were only observed as local defects in $\beta2$ structure [35]. The surface reconstruction with As-rich $\beta2(2\times4)$ is thus adopted as ideal model throughout this work.

All the above results have motivated the present study. Theoretical modeling of the thiolate adsorbed on semiconductor surfaces can provide valuable information for understanding the bonding nature, ultimately, help us to design and optimize a semiconductor-thiolate interface addressing specific applications. In this contribution, we will introduce first-principle calculations to determine the preferred adsorption sites for MT on an oxide-free GaAs (001), and probe more deeply into the nature of the bonding to complement experimental results. In this work, MT, rather than methylthiol (being really used in the experiments), is adopted because it is a very good starting point for studying more complicated systems like long-chain alkylthiols with different ending functional groups like COOH, OH, or SH [20, 36].

Computational framework

All DFT calculations were performed in DMol^3 code [37, 38], the generalized gradient approximation (GGA) with the Perdew–Burke–Emzerhof exchange–correlation functionals (PBE) approach and double numerical plus polarization (DNP) atomic orbitals were taken as basis sets [39]. PBE provides better accuracy than local density approximation (LDA) in description of polar surfaces [40], such as GaAs (001) [15]. The DFT semicore pseudopotentials (DSPP) treatment was implemented for relativistic effects, which replaces core electrons by a single effective potential. The k-point was set to $6 \times 4 \times 1$ for all slabs, which has the convergence tolerance of energy of 2.0×10^{-5} hartree (1 hartree = 27.2114 eV) with the maximum force of 0.004 hartree. For comparison, the identical simulation parameters were employed in all simulations. The bulk lattice constant of GaAs calculated is 5.734 Å and cohesive energy is 6.326 eV, which are consistent with other theoretical values of 5.92 Å and 6.43 eV by GGA+PW91 and 5.51 Å and 8.58 eV by LDA [41]. In addition, our calculations also correspond to present experimental values of 5.65 Å and 6.52 eV [42]. The observed overestimation of lattice constant and deviation of cohesive energies are common for all GGA calculations. The periodic supercell approach was employed to model GaAs (001) surface. The used $\beta2(2\times4)$ structure (8.1×16.2 Å^2) is large enough to avoid interaction between the adjacent thiolates, and potential calculation errors. This (2×4) surface structure corresponds to As coverage of 0.75 and is characterized by two As–As dimers and two missing dimers in the (110) direction on the topmost layer. The second-layer Ga atoms lying beneath the two As dimers are also missing, more specifically, As atoms in the third layer forming dimers [24, 43]. Dimerization of As atoms with the lengths of 2.503 and 2.522 Å, respectively, are found to stabilize the system by energetic drop of 1.50 eV in comparison with the unreconstructed surface. This modeling slab consists of seven atomic layers with the rear surface saturated with H atoms, where the number of H atoms are chosen to satisfy such that the number of non-bonding electrons equals twice the number of 3-fold

coordinated As atoms. As results, partial bulk atoms have 3- or 4-fold coordination configurations [44]. Then, the slab is separated by a vacuum (16 Å thickness) to avoid spurious interactions. The bottommost layer of As atoms along with H-layer were fixed during the geometry optimization, while the rest atoms were allowed to relax. The use of hydrogen termination is necessary due to the polar nature of the (001) surface [45]. Additional tests show that more layers and special k points do not change our conclusions significantly.

The equilibrium geometries, obtained from the first geometry optimization starting from a thiolate with the coverage of 0.125 ML, stand upright above the reconstructed surface in the x–y plane, respectively. The substrate atoms and MT are fully relaxed by minimizing the total energy of the system to get the local most stable sites shown in Fig. 1. This procedure should reveal the possibility of stable adsorption sites for MT [46]. The electronic structures for the adsorption structure and the free MT including molecular orbitals, electron density difference, density of state and Mulliken population analysis, are also calculated under the same accuracy to explain the bond property for MT/GaAs (001) system.

The MT/GaAs (001) binding energies, E_{ad}, were calculated as a difference between the total energy of the slab-adsorbate system and the energies of the substrate GaAs (001) surface and adsorbate MT in gas phase,

$$E_{ad} = E_t - (E_{slab} + E_{mole}) \quad (1)$$

where the subscripts t, slab, and mole denote the total amount of the considered system and the corresponding *clean* slabs and *free* MTs [47]. Spin polarization was included in all binding energy calculations.

Results and discussion

Table 1 and Fig. 1 summarize E_{ad} values and representative geometric parameters obtained for different MT adsorption sites, where L is the distance between the sulfur and the surface atom, and θ is defined as the angle of C–S–Ga or C–S–As bonds. While we only consider the potential energy surfaces for MT adsorption as a function of S position, the characteristics of the MT–Ga are quite different from the MT–As interaction. In the cases of Ga1 and Ga2 in Fig. 1 for Ga, MT is bound to threefold-coordinated second-layer Ga atoms with $E_{ad} = -2.79$ eV without presence of broken As–As dimers, as shown in Table 1. In this case, the surface Ga atom lifts in the direction of changing hybridization from sp^2 to sp^3, which means an accumulation of charge on Ga [48]. On the other hand, As1 in Fig. 2 shows the interaction with the topmost As dimers, where Ga–Ga dimers are formed with As–Ga bond breaking and $E_{ad} = -2.11$ eV. These numerical values agree well with the theoretical data for thiolate on As-rich (2×1) reconstructed surface [15]. The difference of bonding energy values between S–Ga and S–As is 0.68 eV, which is consistent with the calculated value (0.61 eV) of atomic S adsorbed on GaAs (100) surface [49]. In fact, the As–S bond disappeared and only the Ga–S bond was observed after annealing the S-covered GaAs surface to 360° [50]. Moreover, the experiment also found that S–CH_3 converts from As site to a stable Ga site at high temperature at GaAs (100) surface [19]. It is also suggested that $E_{ad} = -1.81$ eV for MT being adsorbed on the topmost As dimers [21] (the most stable structure), which is a little smaller than our value due to possibly the existence of H atom on the adjacent Ga atom [21]. For MT adsorbed on

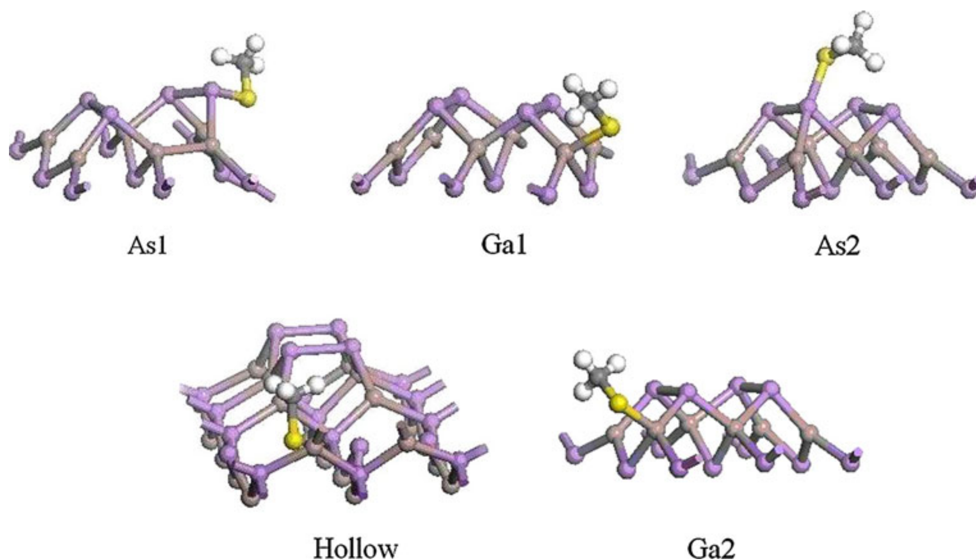

Fig. 1 The final equilibrium structures for the different sites of MT adsorption on GaAs (001)$-\beta2(2\times4)$ surface. As and Ga atoms are represented by *slight gray* (*purple*) and *deeply gray* (*brown* at middle layer) spheres, respectively (Color figure online)

Table 1 E_{ad} in eV and geometrical parameters for the different adsorption configurations studied in Fig. 1. As′ denotes the referenced values [46]

Site	As1	Ga1	As2	Hollow	Ga2	As′
E_{ad}	−2.11	−2.79	−1.56	−1.78	−2.79	−3.75
L	2.35	2.26	2.33	2.70	2.26	2.32
θ	101.85°	99.67°	97.92°	–	100.73°	110.2°
Mulliken	−0.117	−0.252	−0.303	−0.283	−0.248	
	0.076	−0.113	−0.148	−0.146	−0.111	

All distances are in Å. For the values of Mulliken, the *first line* denotes those before MT adsorbed while the second does those after MT adsorbed

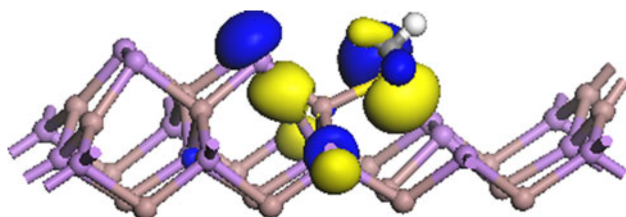

Fig. 2 High lying molecular orbitals of thiolate chemisorbed on GaAs (001) surface at Ga2 site. Isodensity surfaces correspond to 0.03 au

As at (3×3) GaAs (100) surface, $E_{ad} = -3.75$ eV, which is larger than the current value [20, 45]. This may be induced by different geometries of GaAs (100) surface. However, our calculated values of L and θ are consistent with those in Ref. [20]. The configuration also indicates that MT adsorption modifies the surface reconstruction a little, which corresponds to the results of alkanethiolate monolayer on GaAs surface [18, 51]. In As2 of Fig. 1, S is located upon the As atom with $E_{ad} = -1.56$ eV where As–As dimers remain with $d_{As\text{–}Ga}$ elongation of over 12%. For Hollow in Fig. 1, MT is perpendicularly located in the hollow site next to the dimer in the third layer, $E_{ad} = -1.78$ eV, and $d_{As\text{–}As}$ increases about 10%.

In the above configuration, the most negative E_{ad} value is −2.79 eV at Ga1 (Ga2) site while the most positive E_{ad} value is −1.56 eV corresponding to As2 site. These regions are separated by channels parallel and perpendicular to the direction of the dimer rows, indicating the mobile barrier for the adsorbed MT to go from the third layer dimers perpendicular to the topmost dimers [52]. Moreover, Ga2 is also the most interesting binding site. In this configuration, the MT is tilted toward the surface with $\theta_{Ga\text{–}S\text{–}C} = 100.73°$ and $d_{Ga\text{–}S} = 2.26$ Å. The S–C molecular axis is tilted 52.90° from the normal, and the methyl group directed nearly parallel toward the neighbor hollow site with an angle being less than 5°. Since $d_{S\text{–}C}$ increases about 0.05 Å, there is a slight interaction between C atom and GaAs (001) surface, which stabilizes this configuration.

There are also numerous similarities between these geometries especially in chemical bonding sites. The bonds of Ga–S or As–S lie along the Ga (As) dangling bond and $\theta_{Ga\text{–}S\text{–}C}$ ($\theta_{As\text{–}S\text{–}C}$) changes from 99.67° (97.92°) to 100.73° (101.85°), close to $\theta_{C\text{–}S\text{–}H} = 96.80°$ in the free thiol [12]. Two unpaired *p*-electrons of S participate in the formation of the bonds with Ga (As) and C, while other two *p*-electrons of S form a lone pair, which is the highest occupied molecular orbital (HOMO) (Fig. 2) perpendicular to the Ga–S–C plane. The *s*-orbitals do not hybridize with *p*-orbitals. As results, Ga–S and S–C bonds formed by the remaining p_y and p_z orbitals tend to form a nearly right angle [15, 48]. The deviation to larger angle values can be explained by the steric repulsion between CH_3 unit and the surface [15]. Since the covalent radius of S (1.02 Å) is close to that of Ga and As atoms (1.26 and 1.19 Å, respectively) [17], such a preference for the bond direction means a high covalency and a high strength of the bond. The shortest $d_{S\text{–}Ga}$ and $d_{S\text{–}As}$ are 2.26 and 2.33 Å, which are shorter than $d_{Au\text{–}S} = 2.50$ Å [11, 52], suggesting stronger binding of thiolate and GaAs than that of thiolate and Au surface.

Electrical surface passivation is critical for GaAs, which faces significant challenge in future device applications. For electrical passivation, each surface atom will likely need to be functionalized for eliminating surface trap states [15]. The lowest unoccupied molecular orbital (LUMO) of GaAs (001) (2×4) surface is related to dangling bonds that are located at threefold-coordinated second-layer Ga atoms [24]. Overlap between S lone pair and the empty Ga dangling bond results in the preferential adsorption of thiolate on Ga [48] and the eliminating of LUMO on Ga, as also shown in Fig. 2. It can be also seen from the density of states (DOS) in Fig. 3. In CASTEP, the valance band maximum (VBM) is simply defined as the Fermi level for semiconductors and insulators, due to the difficulty that DFT determines the Fermi level for the nonmetallic systems [53–55]. DOS shows that S states nearly have no interaction with Ga states above E_f (Fig. 3(1)), while S-*p* state obviously overlaps with As-*p* and As-*d* states above E_f (Fig. 3(2)). It seems that MT is good for electrical passivation of Ga atoms but not As atoms [21].

The different behaviors of Ga and As interaction with S in MT due to their distinct bonding natures can be seen from DOS. The Ga–S bond is formed mainly through S-*p* orbital hybridizing with both Ga-*s* and Ga-*p* orbitals, while As–S bond is formed mainly through S-*p* orbital hybridizing with As-*p* and S-*s* orbital hybridizing with As-*s* orbital. Obviously, the *s*-orbitals nearly do not hybridize with *p*-orbitals, which are in agreement with the values of $\theta_{Ga\text{–}S\text{–}C}$ and $\theta_{As\text{–}S\text{–}C}$ as discussed above.

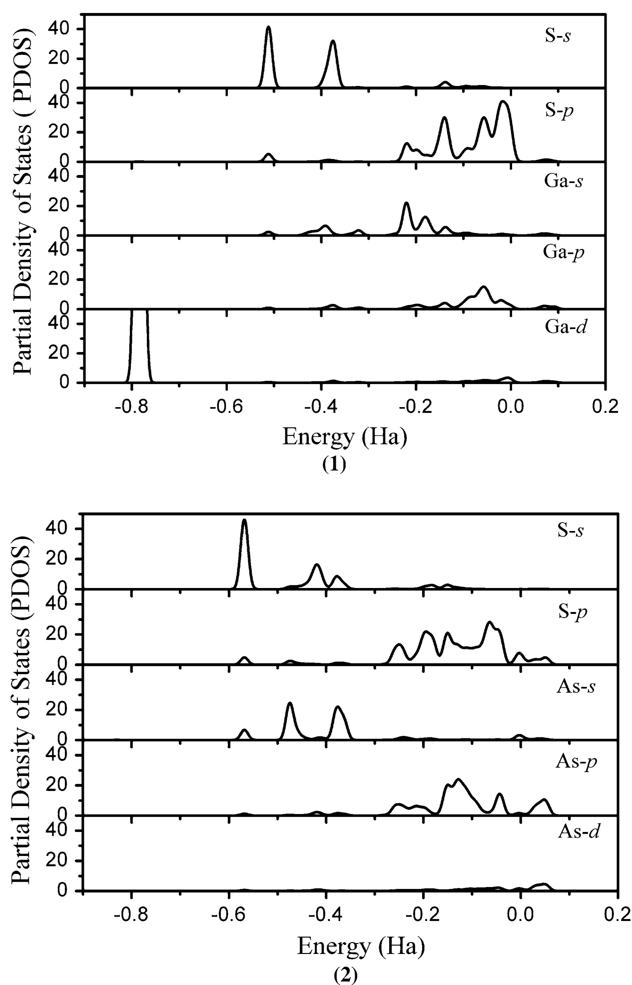

Fig. 3 The partial density of states (PDOS) of S, Ga, and As atoms in adsorbed structures. (1) and (2), respectively, indicate the MT adsorbed structures at Ga2 and As2 sites

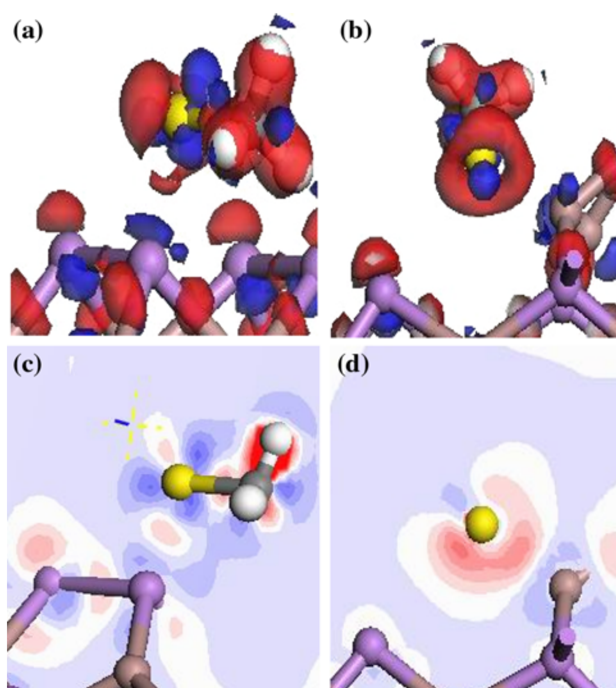

Fig. 4 The plots of the electron density difference. **a** and **b**, respectively, indicate the MT adsorbed structures at Ga2 and As2 sites while **c**, **d** present the slices of **a**, **b**

To evaluate the intensities of Ga–S and As–S bonds, the plots of the electron density difference calculated are shown in Fig. 4. The gray (red) region shows the electron accumulation, while black (blue) region shows the electron loss. The denser the color is, the more the electron density changes. These head group interactions are of importance in controlling interfacial electrical properties on substrates. It can be observed from Fig. 3 that some electrons are accumulated between S and Ga atoms while lesser electrons accumulate between S and As atoms. This means that both S–Ga and S–As bonds have covalent components. Moreover, S–Ga bond is preferred, resulting from the overlap of an S lone pair orbital with an empty Ga dangling bond [48], where a stronger covalent S–Ga bond is built compared with S–As bond. From a thermodynamic viewpoint, the former is energetically more favorable, as found in inorganic sulfides bonding to the group III atom [17], and even MT on a GaAs (100) surface [19].

For qualitative description of the charge transfer, the Mulliken population analysis is performed and shown in Table 1. The initial Mulliken population value of free MT is -0.001 (the calculation error), while that of S is -0.205. Electron density of about 0.1 is depleted in the second-layer Ga dangling bond region in sites As1, Ga1, Ga2, compared with 0.3 for MT on Au surfaces [7]. This feature can be understood on the basis of simple electron-counting arguments, showing a formation of the lower ionicity and higher covalency of the Ga–S bonds. As results, there is a small amount of electron (about 0.6) transfer from methyl group to S. The redistribution of electron density along S–C bond suggests weakening of covalency of C–S bond upon adsorption. In site B2 interacted with the topmost As, the electrons transfer 0.13 from surface to MT, the same magnitude order compared with Ga–S interaction. However, sites As1 also interact with the topmost As with a net excess charge of ~ 0.07 transfer from MT to surface. Since the electrons transfer of 0.01 from methyl groups to S is small, covalency of the C–S bond is only weakened slightly. The trend of S–C length also confirms our conclusion.

Conclusion

In summary, we have investigated the adsorption of MT on an As-rich GaAs (001) surface using DFT. Small charge

transfer between thiolate and surface, and short S–Ga and S–As bond lengths, indicate a highly covalent nature of the bonding. Although the bond strength of S–Ga for thiolate chemisorbed on the surface is comparable to that of S-As, thiolate has a preferred binding to Ga empty bonds on an ideally reconstructed surface. The effective binding to each surface atom are helpful to elucidate the SAMs property of organosulfur compounds.

Acknowledgements The authors acknowledge support by National Key Basic Research and Development Program (Grant No. 2010CB 631001).

References

1. Aqua T, Cohen H, Vilan A, Naaman R (2007) J Phys Chem C 111:16313
2. Adlkofer K, Tanaka M (2001) Langmuir 17:4267
3. Yi SI, Kruse P, Hale M, Kummel AC (2001) J Chem Phys 114:3215
4. Shaporenko A, Adlkofer K, Johansson LSO, Tanaka M, Zharnikov M (2003) Langmuir 19:4992
5. McGuiness CL, Shaporenko A, Mars CK, Uppili S, Zharnikov M, Allara DL (2006) J Am Chem Soc 128:5231
6. Lee K, Lu G, Facchetti A, Janes DB, Marks TJ (2008) Appl Phys Lett 92:123509
7. Nesher G, Vilan A, Cohen H, Cahen D, Amy F, Chan C, Hwang J, Kahn A (2006) J Phys Chem B 110:14363
8. Li WJ, Kavanagha KL, Talin AA, Clift WM, Matzke CM, Hsu JWP (2007) J Appl Phys 102:013703
9. Gassull D, Ulman A, Grunze M, Tanaka M (2008) J Phys Chem B 112:5736
10. Lavrich DJ, Wetterer SM, Bernasek SL, Scoles G (1998) J Phys Chem B 102:3456
11. Pontes RB, Novaes FD, Fazzio A, da Silva AJR (2006) J Am Chem Soc 128:8996
12. Schreuber F (2000) Prog Surf Sci 65:151
13. Sheen CW, Shi JX, Martensson J, Parikh AN, Allara DL (1992) J Am Chem Soc 114:1514
14. Adlkofer K, Eck W, Grunze M, Tanaka M (2003) J Phys Chem B 107:587
15. Voznyy O, Dubowski JJ (2006) J Phys Chem B 110:23619
16. Donev S, Brack N, Paris NJ, Pigram PJ, Singh NK, Usher BF (2005) Langmuir 21:1866
17. McGuiness CL, Shaporenko A, Zharnikov M, Walker AV, Allara DL (2007) J Phys Chem C 111:4226
18. Zhou CZ, Walker AV (2008) J Phys Chem C 112:797
19. Huang TP, Lin TH, Teng TF, Lai YH, Huang WH (2009) Surf Sci 603:1244
20. Saavedra M, Buljan A, Munoz M (2009) J Mol Struct Theochem 906:72
21. Lebedev MV (2008) Semiconductors 42:1048
22. Hashizume T, Xue QK, Zhou J, Ichimiya A, Sakurai T (1994) Phys Rev Lett 73:2208
23. Hashizume T, Xue QK, Zhou J, Ichimiya A, Sakurai T (1995) Phys Rev B 51:4200
24. Schmidt WG, Bechstedt F (1996) Phys Rev B 54:16742
25. Schmidt WG, Mirbt S, Bechstedt F (2000) Phys Rev B 62:8087
26. Ohtake A, Ozeki M, Yasuda T, Hanada T (2002) Phys Rev B 65:165315
27. Laukkanen P, Kuzmin M, Perälä RE, Ahola M, Mattila S, Väyrynen IJ, Sadowski J, Konttinen J, Jouhti T, Peng CS, Saarinen M, Pessa M (2005) Phys Rev B 72:045321
28. Ohtake A (2006) Phys Rev B 74:165322
29. Farrell HH, Palmstrøm CJ (1990) J Vac Sci Technol B 8:903
30. Laukkanen P, Perälä RE, Vaara RL, Väyrynen IJ, Kuzmin M, Sadowski J (2004) Phys Rev B 69:205323
31. Garreau Y, Sauvage-Simkin M, Jedrecy N, Pinchaux R, Veron MB (1996) Phys Rev B 54:17638
32. LaBella VP, Bullock DW, Emery C, Ding Z, Thibado PM (2001) Appl Phys Lett 79:3065
33. Lee SH, Moritz W, Sheffler M (2000) Phys Rev Lett 85:3890
34. Schmidt WG (2002) Appl Phys A 75:89
35. Ohtake A (2008) Surf Sci Rep 63:295
36. Jiang P, Liu ZF, Cai SM (2002) Langmuir 18:4495
37. Delley B (1990) J Chem Phys 92:508
38. Delley B (2000) J Chem Phys 113:7756
39. Perdew JP, Burke K, Ernzerhof M (1996) Phys Rev Lett 77:3865
40. Miotto R, Srivastava GP, Ferraz AC (1999) Phys Rev B 59:3008
41. Juan YM, Kaxiras E (1993) Phys Rev B 48:14944
42. Cohen ML, Chelikowsky JR (1988) Electronic structure and optical properties of semiconductors. Springer, New York
43. Srivastava GP, Jenkins SJ (1996) Phys Rev B 53:12589
44. Fu Q, Li L, Hicks RF (2000) Phys Rev B 61:11034
45. Moll N, Kley A, Pehlke E, Scheffler M (1996) Phys Rev B 54:8844
46. Bonapasta AA (2002) Phys Rev B 65:045308
47. Liu W, Lian JS, Jiang Q (2007) J Phys Chem C 111:18189
48. Voznyy O, Dubowski JJ (2008) J Phys Chem C 112:3726
49. Ohno T (1991) Phys Rev B 44:6306
50. Sugahara H, Oshima M, Shigekawa H, Nanichi Y (1989) Abstract of 21st conference on the solid state devices and materials. The Japan Society of Applied Physics, Tokyo, p 547
51. McGuiness CL, Blasini D, Masejewski JP, Uppili S, Cabarcos OM, Smilgies D, Allara DL (2007) ACS Nano 1:30
52. Bent SF (2007) ACS Nano 1:10
53. Engels B, Richard P, Schroeder K, Blügel S, Ebert Ph, Urban K (1998) Phys Rev B 58:7799
54. Perdew JP, Levy M (1983) Phys Rev Lett 51:1884
55. Rutter MJ, Robertson J (1998) Phys Rev B 57:9241